

Are your **MRI contrast agents** cost-effective?

Learn more about generic **Gadolinium-Based Contrast Agents**.



**FRESENIUS
KABI**

caring for life

AJNR

3D C-Arm Conebeam CT Angiography as an Adjunct in the Precise Anatomic Characterization of Spinal Dural Arteriovenous Fistulas

T.D. Aadland, K.R. Thielen, T.J. Kaufmann, J.M. Morris, G. Lanzino, D.F. Kallmes, B.A. Schueler and H. Cloft

This information is current as of April 17, 2024.

AJNR Am J Neuroradiol 2010, 31 (3) 476-480

doi: <https://doi.org/10.3174/ajnr.A1840>

<http://www.ajnr.org/content/31/3/476>

**ORIGINAL
RESEARCH**

T.D. Aadland
K.R. Thielen
T.J. Kaufmann
J.M. Morris
G. Lanzino
D.F. Kallmes
B.A. Schueler
H. Cloft

3D C-Arm Conebeam CT Angiography as an Adjunct in the Precise Anatomic Characterization of Spinal Dural Arteriovenous Fistulas

BACKGROUND AND PURPOSE: Precise anatomic understanding of the vascular anatomy of SDAVFs is required before treatment. This study demonstrates the utility of C-arm conebeam CT to locate precisely the fistulous point in SDAVFs and the courses of their feeding arteries and draining veins.

MATERIALS AND METHODS: This retrospective study reports 14 consecutive patients with SDAVFs who underwent DSA and C-arm conebeam CT angiography. SDAVF sites included 5 thoracic, 7 lumbar, and 2 sacral fistulas. Selective DSA initially identified the location and arterial supply of the SDAVF. C-arm conebeam CT angiography was then performed with selective injection into the feeding artery. Reconstructed images were reviewed at a workstation with the referring surgeon, in conjunction with the standard 2D DSA images. The value of C-arm conebeam CT in depicting the fistula and the relationship to adjacent structures was qualitatively assessed.

RESULTS: In all 14 patients, C-arm conebeam CT angiography was technically successful and precisely demonstrated the site of the fistula, feeding arteries, draining veins, and the relationship of the fistula to adjacent osseous structures. Information obtained from the C-arm conebeam CT angiogram was considered useful in all surgically (12 patients) and endovascularly (2 patients) treated SDAVFs.

CONCLUSIONS: 3D C-arm conebeam CT angiography is a useful adjunct to 2D DSA in the anatomic characterization of SDAVFs. The technique allowed improved visualization of the vascular anatomy of the SDAVFs and clearer definition of their spatial relationships to adjacent structures.

ABBREVIATIONS: AP = anteroposterior; AV = arteriovenous; DSA = digital subtraction angiography; MPR = multiplanar reformation; SDAVF = spinal dural arteriovenous fistula

SDAVFs represent a specific subtype of spinal vascular malformation in which an arteriovenous fistula is located typically within the dura mater of a nerve root sleeve, underneath the vertebral body pedicle in the neural foramen.¹ Such a fistula is supplied by a radiculomeningeal artery, which normally supplies the dural root sleeve and adjacent spinal dura, and drains via an adjacent radicular vein.² This arteriovenous shunt substantially increases the vascular pressure of the radicular vein, and this increased pressure is transmitted retrograde to the superficial longitudinal median spinal cord veins and to the intrinsic spinal cord veins, which would otherwise drain by this “arterialized” radicular vein.^{3,4} The shunt results in venous hypertension in the spinal cord, decreased arterial perfusion, spinal cord ischemia, and ultimately infarction.⁵ Most SDAVFs are solitary, and >90% are located in the thoracolumbar region. SDAVFs are much less common in the cervical (2%) and sacral (4%) spine.⁵

Precise localization and anatomic delineation of the fistula site remain challenging despite conventional catheter spinal angiography, MR imaging/MR angiography, and high-resolution CT imaging. Conventional DSA is the current standard for pretherapy imaging and has high spatial resolution, but it is necessarily limited by its planar imaging nature. Combining the tomographic or volumetric nature of CT with the small

vascular structure opacification that is obtained with selective conventional angiography would be ideal for showing relationships between SDAVFs and adjacent anatomic structures, and this is now possible with the advent of conebeam CT angiography.

We present a series of 14 patients with SDAVF, in which an Artis zee biplane angiographic system (Siemens Medical Solutions, Erlangen, Germany) was used to perform conventional catheter 2D DSA and 3D conebeam CT angiography during intra-arterial injection for improved localization and anatomic clarification of the SDAVFs.

Materials and Methods

Institutional review board approval was obtained for this study. Between May 2008 and March 2009, a total of 14 patients (12 men and 2 women; age range, 51–85 years; mean, 65.9 ± 9.7 years) at a single institution were confirmed to have SDAVFs. The SDAVF sites included 5 thoracic, 7 lumbar, and 2 sacral fistulas. Following localization of the SDAVFs and identification of their arterial supply with conventional 2D DSA, we performed catheter-based rotational conebeam volume CT during selective arterial contrast iohexol (Omnipaque 300; GE Healthcare, Princeton, New Jersey) injection through the catheter into the feeding segmental or iliac artery, either manually administered by using a syringe or by using a power injector. Depending on the level of the SDAVF, the volume and injection rate of contrast material was determined on the basis of injections performed previously for the DSA. The SDAVF feeding artery was fully opacified, and the draining vein was clearly identified during the 3D conebeam CT acquisition. Examples of contrast material volumes and injection rates by catheter tip locations include the following: internal iliac

Received May 11, 2009; accepted after revision July 21.

From the Departments of Radiology (T.D.A., K.R.T., T.J.K., J.M.M., D.F.K., B.A.S., H.C.) and Neurosurgery (G.L.), Mayo Clinic, Rochester, Minnesota.

Please address correspondence to Kent R. Thielen, MD, Department of Radiology, Mayo Clinic, 200 1st St SW, Rochester, MN 55905; e-mail: thielen.kent@mayo.edu

DOI 10.3174/ajnr.A1840

arteries, 12.0 mL at 2.0 mL/s; and intercostal or lumbar arteries, 6.0 mL at approximately 1.0 mL/s by hand injection.

Imaging parameters for the 3D C-arm conebeam CT acquisitions were as follows: Projection images were acquired with an Artis zee biplane system by using a 30 × 40 cm flat panel detector. Image acquisition covered 100°, left anterior oblique to 100° right anterior oblique in a propeller axis rotation of the C-arm with the x-ray tube traveling under the patient. The total acquisition time was 8 seconds for 397 projection images, by using the 360-mGy/frame dose mode. Only a single conebeam CT acquisition was obtained for each case. The effective radiation dose per conebeam CT acquisition ranged from 7.8 to 12.1 mSv with a mean of 9.9 mSv. In comparison, a typical radiation dose for conventional DSA spinal angiography is 1.0 mSv for AP, 3.0 mSv for oblique, and 6.0 mSv for lateral series acquisitions. The arterial injection for the conebeam CT angiogram was timed to allow both arterial and venous opacification throughout the acquisition. MPRs were performed by using an external postprocessing workstation (syngo X Workplace; Siemens Medical Solutions) to produce sections with 0.27- to 0.44-mm pixel size and a section thickness of 0.27–0.44 mm.

MPRs with variable section thicknesses were reviewed by the neuroradiologist at the workstation, including in the sagittal and coronal planes. Before surgical intervention, the neuroradiologist who performed the combined spinal angiography/3D C-arm conebeam CT reviewed the 3D dataset on an external postprocessing workstation (syngo X Workplace) with the neurosurgeon. If embolization was chosen as a treatment, the neuroradiologist reviewed the volumetric dataset from either the external postprocessing workstation or the intraprocedure monitors.

Results

In all 14 patients, 3D C-arm conebeam CT clearly demonstrated the feeding artery, the fistula site, and the draining veins. In addition, the anatomic landmarks in relation to the fistula were clearly delineated. The precise location of the fistula relative to the adjacent osseous anatomy, such as the adjacent vertebral body pedicle, was particularly helpful to the neurosurgeons in surgical planning and was considered easier to visualize relative to standard 2D DSA images. The draining radicular vein could be followed in all cases from the fistula site to the coronal venous plexus around the spinal cord, and the dural entry point of the radicular vein was estimated for each case. The information obtained from the 3D C-arm conebeam CT angiogram was considered useful in treatment planning for all surgically treated SDAVFs (12 patients) and for all endovascularly glue-embolized (1, 3-bis [2-chloroethyl]-1-nitrosourea) SDAVFs (2 patients). In all 14 cases, the SDAVF was considered to be better delineated in terms of anatomic location with the 3D C-arm conebeam CT angiography dataset than with the conventional spinal 2D DSA.

Representative Cases

Case 1. A 56-year-old man presented with a 1-year history of episodic and progressive bilateral lower limb weakness with paresthesias and a sense of “warmth” involving the bilateral lower limbs. Review of the MR imaging showed a nonenhancing parenchymal T2 hyperintensity in the spinal cord, extending from T5 through the conus, with mild cord expansion. Prominent curvilinear signal-intensity voids were seen dorsal to the thoracic cord.

Bilateral T5-T8 selective spinal angiography was performed along with T7 biplane and 3D C-arm conebeam CT angiography with MPR images, which demonstrated an SDAVF located along the undersurface of the left T7 pedicle, which was supplied by the radiculomeningeal artery arising from the left T7 intercostal artery (Fig 1).

The fistula was surgically obliterated. A follow-up MR imaging approximately 3 months status postsurgery showed that the swelling and T2 hyperintensity within the cord had mildly decreased, and the serpiginous flow voids dorsal to the cord had resolved. At 3 months, the patient felt that his legs were stronger, and he could now exercise for 2 hours without noticeable weakness. He still had some burning discomfort in his legs, but he felt that it was not severe enough to take any type of medication.

Case 2. A 54-year-old woman was healthy until the spring of 2007, when she began to trip and fall on uneven ground. A spinal MR imaging and conventional spinal angiogram suggested a SDAVF.

Biplane DSA and 3D C-arm conebeam CT angiography demonstrated a dural AV fistula in the sacral spine, arising from a lateral sacral branch, which extended through the left S1 foramen (Fig 2). The operating neurosurgeons reported a significant increase in their understanding of the location and anatomy of the SDAVF after reviewing the 3D conebeam CT angiogram on the workstation. The fistula was then surgically obliterated. A follow-up angiogram 5 days later showed no evidence of a residual dural AV fistula, and a follow-up MR imaging approximately 4 months later showed complete resolution of both the abnormal spinal cord signal intensity and prominent flow voids distal to the cord. At 4 months, the patient had mild improvement with stable walking capability and improved bladder control.

Case 3. A 76-year-old man was transferred from an outside hospital for further evaluation regarding lower extremity weakness and urinary retention that had been present and progressive for 5 weeks. The lower extremity weakness gradually worsened to the point that he could not ambulate on his own and required 2-person assistance. The patient denied any episodes of upper or lower extremity weakness in the past. MR imaging of his thoracic spine performed at the outside institution before transfer showed subtle increased T2 signal intensity within the inferior aspect of the spinal cord from T9 to T12 and abnormal vascularity along the dorsal aspect of the thoracic cord, suspicious for a SDAVF.

MR angiography of the entire spine with intravenous gadolinium was performed at our institution and showed a prominent vessel entering the spinal canal beneath the left T12 pedicle, with an ascending vein that drained superiorly into multiple prominent pial vessels along the dorsal aspect of the spinal cord, extending superiorly to T1. AP digital subtraction and 3D C-arm conebeam CT angiograms, acquired with injections of the left T12 radicular artery, demonstrated a dural arteriovenous fistula beneath the left T12 pedicle with an arterialized vein entering the spinal canal along the root sleeve (Fig 3). A posterior spinal artery also originated from this radicular artery, which precluded embolization. The patient was taken to surgery for disconnection of the fistula. After opening the dura, the surgeon identified 2 parallel ascending vessels. The draining vein was arterialized, and it was difficult to dif-

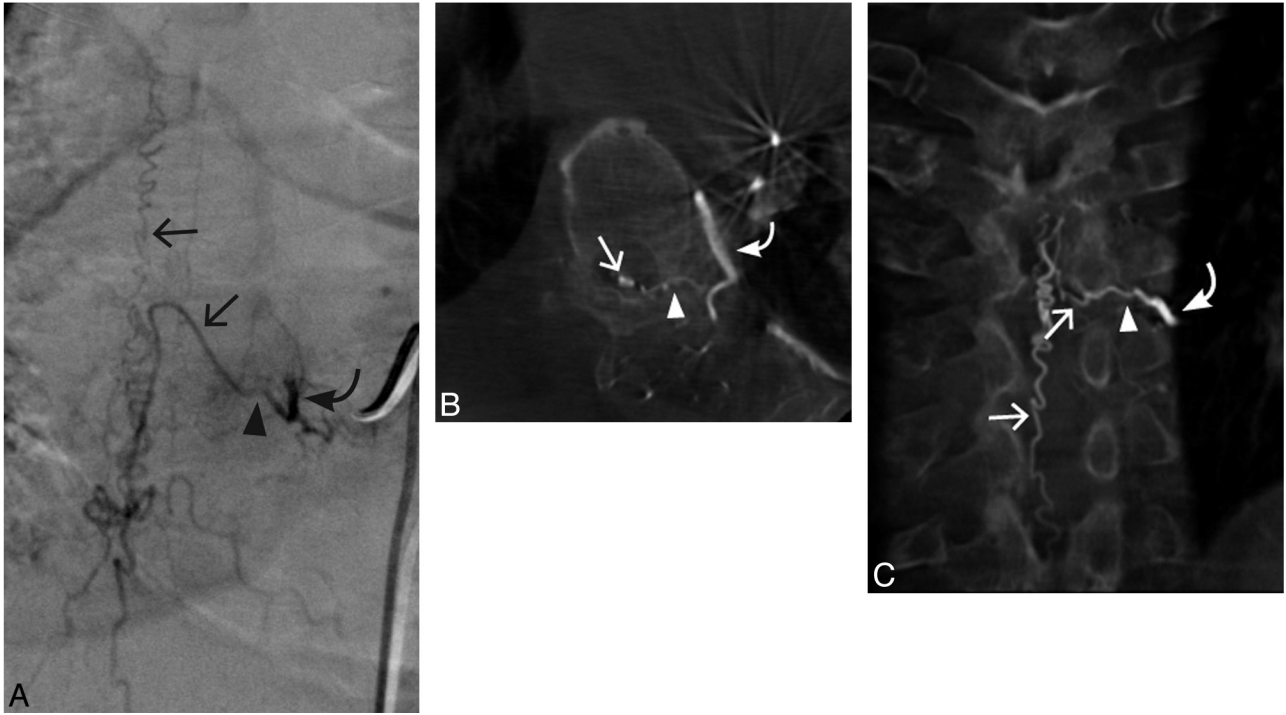


Fig 1. Case 1. A 56-year-old man with a left T7 SDAVF. *A*, Conventional DSA AP view. *B*, 3D C-arm conebeam axial MPR CT angiogram. *C*, 3D C-arm conebeam coronal MPR CT angiogram. Curved arrows indicate the arterial supply to the SDAVF; arrowheads, the fistulous point of the SDAVF; straight arrows, arterialized veins draining the SDAVF.

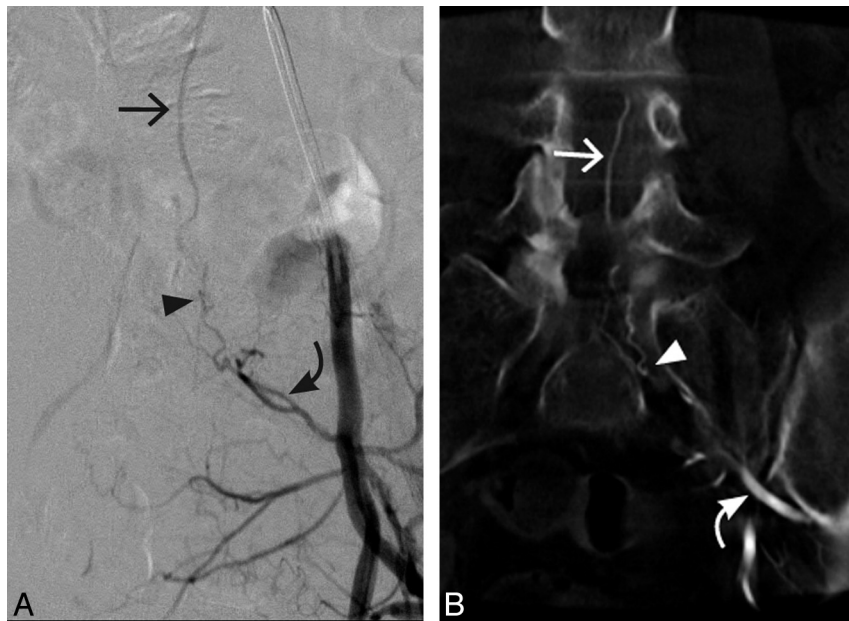


Fig 2. Case 2. A 54-year-old woman with an SDAVF arising from a left lateral sacral branch extending through the left S1 foramen. *A*, Conventional DSA AP view. *B*, 3D C-arm conebeam coronal MPR CT angiogram. Curved arrows indicate the arterial supply of the SDAVF; arrowheads, the fistulous point of the SDAVF; straight arrows, the arterialized veins draining the SDAVF.

ferentiate from the posterior spinal artery. In this case, the 3D C-arm conebeam CT was also helpful in clarifying the mutual anatomic relationship between the artery and the vein. Three weeks after surgical interruption of the fistula, the patient was able to ambulate with a walker.

Discussion

We have found spinal 3D C-arm conebeam CT angiography to be a powerful adjunct to conventional 2D catheter-

based angiography in the localization and anatomic depiction of SDAVFs. Use of catheter-based 3D C-arm conebeam CT may provide spinal angiographers and physicians contemplating therapeutic interventions a significantly enhanced and more precise understanding of the vascular anatomy of SDAVFs and their relationship to adjacent anatomic structures. This information should aid in focusing endovascular or surgical therapies for SDAVFs.

The efficacy of 3D C-arm conebeam CT angiography in the

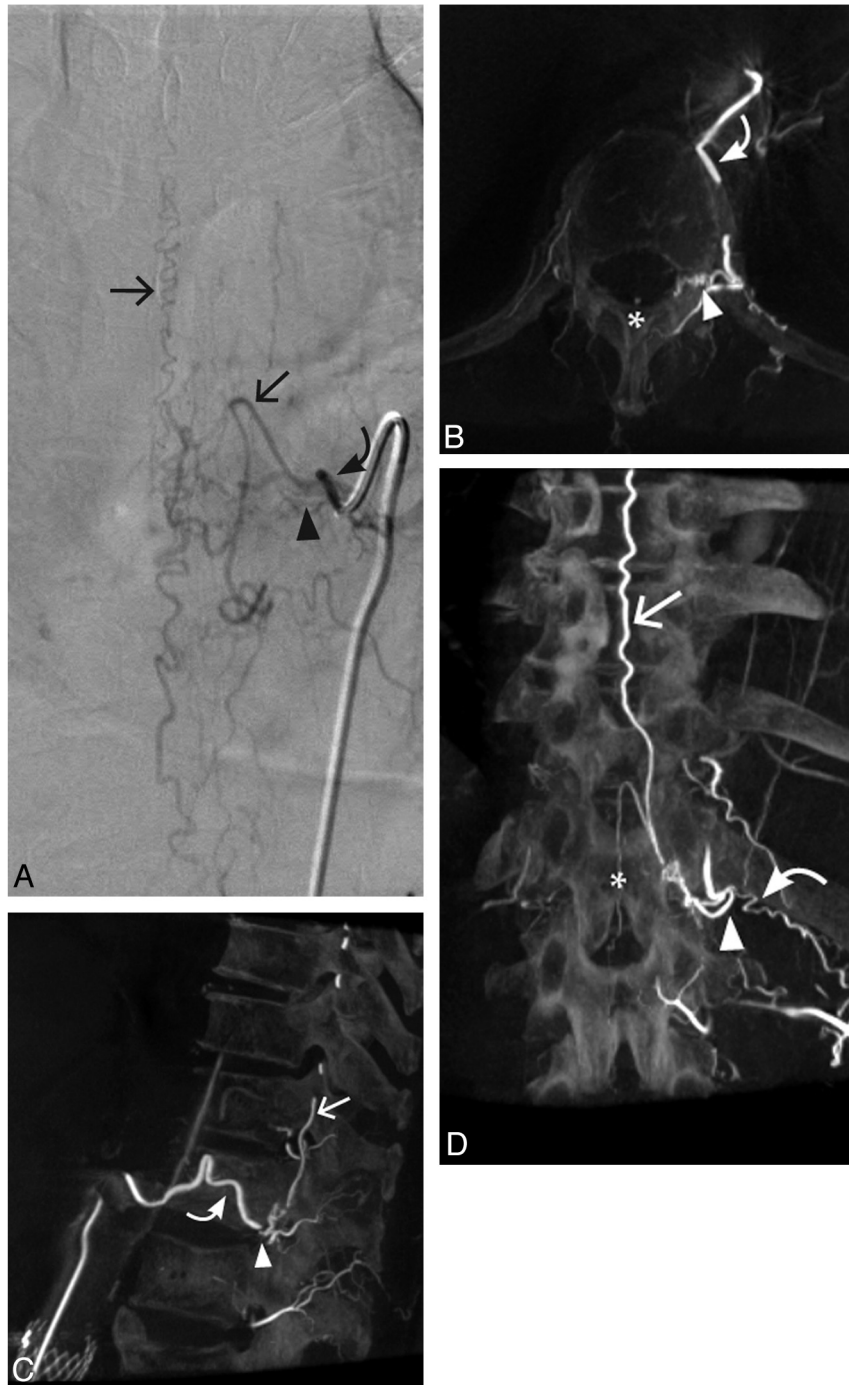


Fig 3. Case 3. A 76-year-old man with a left T12 SDAVF. *A*, Conventional DSA AP view. *B*, 3D C-arm conebeam axial MPR CT angiogram. *C*, Sagittal 3D C-arm conebeam MPR CT angiogram. *D*, 3D C-arm conebeam coronal MPR CT angiogram. Curved arrows indicate the arterial supply of the SDAVF; arrowheads, the fistulous point of the SDAVF; straight arrows, the arterIALIZED veins draining the SDAVF; asterisk, the posterior spinal artery.

detection of the fistulous point of cerebral dural arteriovenous fistulas has recently been reported.⁶ Two case reports have described single cases using 3D C-arm conebeam CT and conventional CT, respectively, in the evaluation of an SDAVF.^{7,8} However, to our knowledge, a case series describing the use of 3D C-arm conebeam CT angiography in conjunction with conventional DSA in the evaluation of SDAVFs has not been heretofore published.

Conventional DSA provides significant diagnostic value for the hemodynamic evaluation of SDAVFs and is part of the

current standard of care. However, obtaining oblique and lateral DSA projections to complement the initial frontal projections requires repeated selective angiographic acquisitions with increased examination times, repeated doses of contrast material, and increased exposure to radiation.⁶ These additional oblique and lateral DSA series have been essentially replaced in our practice with a single 3D conebeam CT angiographic acquisition. Catheter-based C-arm conebeam CT angiography provides the 3D information that is otherwise sought with multiple oblique and lateral 2D DSA projections,

but with easier and clearer depiction of the components of the fistulas and their relationships in space to osseous and neural anatomy. The high contrast resolution, high spatial resolution, and isotropic voxels of 3D C-arm conebeam CT allow quality multiplanar reconstructions that easily depict the fistulas and their spatial relationships.

Our study has several limitations. The study was conducted retrospectively; thus, it was subject to bias. Although this study is the largest, to our knowledge, of this specific group of patients with SDAVFs imaged with 3D C-arm conebeam CT, it still involved a relatively small group of patients. In addition, the 3D C-arm conebeam CT digital angiograms were not compared with those of 3D DSA. The study provides good evidence that 3D C-arm conebeam CT angiography can be a useful adjunct in the evaluation of patients with SDAVF. Finally, 3D C-arm conebeam CT does not provide dynamic visualization of the flow within the SDAVF vascular structures. Therefore, interpretation in conjunction with the 2D DSA images is required to assist in distinguishing feeding arteries from draining veins.

Conclusions

In this study, 3D C-arm conebeam CT angiography was a useful adjunct to 2D DSA in the anatomic characterization of

SDAVFs. The technique allowed improved visualization of vascular anatomy of the SDAVFs and clearer definition of their spatial relationships to adjacent structures.

References

1. Farb RI, Kim JK, Willinsky RA, et al. **Spinal dural arteriovenous fistula localization with a technique of first-pass gadolinium-enhanced MR angiography: initial experience.** *Radiology* 2002;222:843–50
2. Park SB, Han MH, Tae-Ahn J, et al. **Spinal dural arteriovenous fistulas: clinical experience with endovascular treatment as a primary therapeutic modality.** *J Korean Neurosurg Soc* 2008;44:364–69
3. Hassler W, Thron A. **Flow velocity and pressure measurements in spinal dural arteriovenous fistulas.** *Neurosurg Rev* 1994;17:29–36
4. Hassler W, Thron A, Grote EH. **Hemodynamics of spinal dural arteriovenous fistulas: an intraoperative study.** *J Neurosurg* 1989;70:360–70
5. Jellema K, Tijssen C, van Gijn J. **Spinal dural arteriovenous fistulas: a congestive myelopathy that initially mimics a peripheral nerve disorder.** *Brain* 2006;129:3150–64
6. Hiu T, Kitagawa N, Morikawa M, et al. **Efficacy of DynaCT digital angiography in the detection of the fistulous point of dural arteriovenous fistulas.** *AJNR Am J Neuroradiol.* 2009;30:487–91. Epub 2009 Feb 12
7. Irie K, Murayama Y, Saguchi T, et al. **DynaCT soft-tissue visualization using an angiographic C-arm system: initial clinical experience in the operating room.** *Neurosurgery* 2008;62(3 suppl 2):266–72
8. Sugawara T, Hirano Y, Itoh Y, et al. **Angiographically occult spinal dural arteriovenous fistula located using selective computed tomography angiography.** *J Neurosurg Spine* 2007;7:215–20